Medical Engineering and Physics 122 (2023) 104072

Contents lists available at ScienceDirect

Medical Engineering and Physics

journal homepage: www.elsevier.com/locate/medengphy

The sensitivity of the stiffness and thickness of a titanium inlay in a cementless PEEK femoral component to the micromotions and bone strain energy density

Corine E. Post [a,*], Thom Bitter [a], Adam Briscoe [b], Nico Verdonschot [a,c], Dennis Janssen [a]

[a] Radboud University Medical Centre, Orthopaedic Research Laboratory, Nijmegen, the Netherlands
[b] Invibio Ltd., Thornton Cleveleys, Lancashire, United Kingdom
[c] University of Twente, Faculty of Engineering Technology, Laboratory for Biomechanical Engineering, Enschede, the Netherlands

ARTICLE INFO

Keywords:
Cementless femoral component
Finite element analysis
Micromotions
Polyetheretherketone
Strain energy density
Titanium inlay

ABSTRACT

Polyetheretherketone (PEEK) has been proposed as alternative material for total knee arthroplasty implants due to its low stiffness, which may reduce stress-shielding. In cementless fixation, a proper primary fixation is required for long-term fixation. Previous research showed that the lower stiffness of a cementless PEEK femoral component results in larger micromotions at the implant-bone interface compared to a cobalt-chrome femoral component. A titanium inlay on the PEEK implant surface may improve the primary fixation while maintaining the favourable stiffness properties. Therefore, the effect of thickness and stiffness of a titanium inlay on the primary fixation and stress-shielding was investigated. A finite element model of the femur and femoral component was created with five titanium inlay variants. The micromotions and strain energy density (SED) were quantified as outcome measures. The distal thin – proximal thick variant showed the largest resulting micromotions (51.2 μm). Relative to the all-PEEK femoral component, the addition of a titanium inlay reduced the micromotions with 30 % to 40 % without considerably affecting the stress-shielding capacity (strain energy difference of 6 % to 10 %). Differences in micromotions (43.0–51.2 μm) and SED between the variants were relatively small. In conclusion, the addition of a titanium inlay could lead to a reduction of the micromotions without substantially affecting the SED distribution.

1. Introduction

While traditional total knee arthroplasty (TKA) components are made of metal alloys such as cobalt-chrome or titanium, high-grade plastics such as ultra-high-molecular-weight polyethylene (UHMWPE) and polyetheretherketone (PEEK) have been proposed as alternative implant materials. PEEK has a lower stiffness than traditional metal alloys, which has the potential benefit of reduced stress-shielding [1]. Stress-shielding could on the long-term lead to loss of bone stock and consequently bone fracture and aseptic loosening of the femoral component [2].

Recent computational studies of cemented femoral components using finite element (FE) analysis show that a PEEK implant leads to a stress distribution in the bone that more closely resembles the situation before prosthesis implantation [1,3,4]. These studies demonstrate that the reduction in stress-shielding for a PEEK femoral component is substantial compared to conventionally used cobalt-chrome alloy (CoCr) femoral components.

While previous studies focused on cemented femoral TKA reconstructions, there is also an interest in cementless fixation via bone ingrowth of PEEK implants, as the survival time of cemented TKA is generally thought to be limited [5–7]. Primary fixation is crucial to ensure a long-term survival of cementless implants. A recent study, however, concluded that a cementless PEEK femoral component leads to larger micromotions at the implant-bone interface compared to a cementless CoCr femoral component [8]. Large micromotions may lead to the formation of a soft tissue layer at the interface, inhibiting long-term fixation through osseointegration.

To improve the primary fixation of cementless femoral components a titanium coating on the inner implant interface can be used [9]. Porous titanium has been widely used for facilitating bone ingrowth and is therefore widely used in cementless implants. A titanium coating can be

* Corresponding author at: Orthopaedic Research Laboratory 620, Geert Grooteplein Zuid 10, 6525 GA Nijmegen, the Netherlands.
E-mail address: corine.post@radboudumc.nl (C.E. Post).

https://doi.org/10.1016/j.medengphy.2023.104072
Received 15 June 2023; Received in revised form 30 October 2023; Accepted 19 November 2023
Available online 20 November 2023

used to optimize the frictional properties of the coating that is in contact with the bone, but by increasing the coating thickness also the structural stiffness of the implant can be adapted. This in turn influences the press-fit fixation and the micromotions at the interface. The titanium coating can be integrated in the PEEK implant through an inlay that is incorporated in the injection moulding process. However, the optimal thickness and stiffness of such an inlay for a press-fit PEEK femoral component is unknown. A too thick inlay would result in the implant losing its potential bone saving capacity, while a too thin inlay would result in no reduction of the micromotions. An implant with an inlay with variable thickness might enhance the primary stability as well as preserving the reducing stress-shielding capacity of the PEEK component. Such variations are quite difficult to investigate in an experimental set-up. Computational modelling, however, provides the opportunity to isolate and simulate the effect of inlay variations on the primary stability.

Therefore, the objective of the current study was to investigate the effect of thickness and stiffness of a titanium inlay on the primary fixation, quantified by the micromotions, and on stress-shielding, quantified by the strain energy density (SED), using finite element analysis.

2. Materials and methods

An FE model of the femur with a femoral component including a titanium inlay was created. Three different inlay thickness variants named thin, medium and thick were considered (Fig. 1). To define the structural stiffness of the titanium inlays, the three different thickness variants were tested in physical three-point bending tests. Subsequently, the thickness and stiffness characteristics of the three inlay variants were used in the FE model.

2.1. Titanium inlays

Five samples of each inlay variant were obtained to define the material properties using a three-point bending test. Each inlay consisted of a solid core and two porous outer layers sintered together (Table 1).

2.2. Experimental three-point bending tests

Three-point bending experiments were performed in an MTS machine (MTS Systems Corporation, Eden Prairie, Minnesota, USA) with a custom-made set-up consisting of a load applicator and two supports, all with a radius of 2 mm. Three-point bending experiments were performed to determine the stiffness properties of the corresponding titanium inlay variant that will be used in the FE models. Before the three-point bending tests, the inlays were milled, painted with white paint and marked with three red dots to facilitate measurement of the deflection using digital image correlation (DIC) (Fig. 2). DIC measurements were used to quantify the small displacements of the inlay instead of the MTS displacements, to avoid measurement errors due to plastic deformation of the porous outer layers. We performed a sensitivity analysis which showed a precision of 95 % for the Young's modulus of the whole system. A 3D printed tool was used to position the inlay on the supports.

At the start of the experiment, the load applicator was positioned on the inlay. Subsequently, one sample was used to define the maximum displacement in the elastic region, in displacement increments of 0.1 mm. Subsequently, all samples were tested at a rate of 2.0 mm/min until the maximum displacement in the elastic region was achieved. A force-displacement curve was created to calculate the average representative Young's modulus per sample (Equation 1). This equation is typically used for a homogeneous material. Although the physical inlays are not homogeneous, it was modelled as a homogeneous material in the FE model. The displacement of the left and right dot was subtracted from the displacement of the central dot. As a final result, the average representative Young's modulus of all 5 samples was taken for the three inlay types.

Table 1
Characteristics of the three inlay variants.

Titanium inlay type	Global thickness (mm)	Thickness solid core (mm)
Thin	1.50	0.25
Medium	1.70	0.50
Thick	2.20	1.00

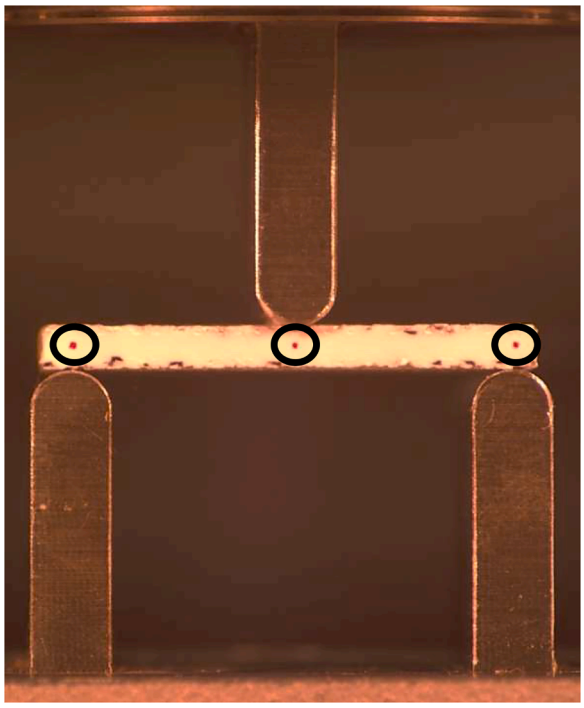

Fig. 2. Overview of the titanium inlay including supports and load applicator. The red dots are indicated with black circles.

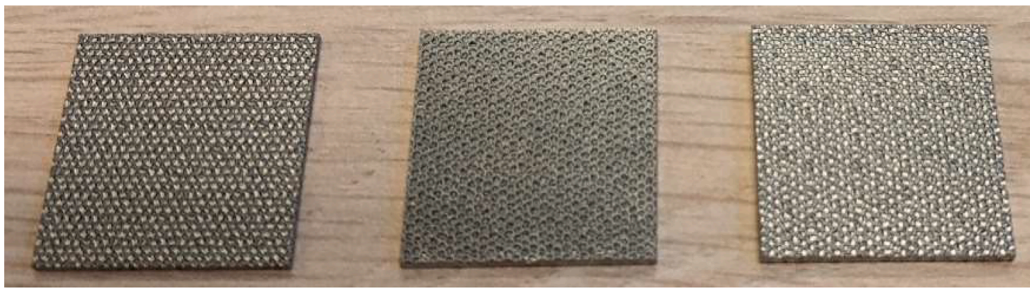

Fig. 1. Thin, medium and thick inlay.

$dP/dw_0 = 48EI/L^3$

$I = a^3b/12$

Equation 1. The gradient between the applied force P and the central displacement w_0 was used to define the average representative Young's modulus E. I = second moment of area, L = support span, a = thickness inlay, b = width inlay.

2.3. FE model

The FE model of a femur implanted with a cementless femoral component from a previous study was used [8]. The CT-scan of a cadaveric right femur (62 years, male) was segmented to create the 3D model of the femur using medical imaging software (Mimics 14.0, Materialise, Leuven, Belgium). An average size C cementless femoral knee component was virtually implanted on the femur (Freedom knee, Maxx Orthopedics, Norristown, PA, USA). The alignment of the implant on the bone was verified by an experienced orthopaedic surgeon. The implant was aligned according to the mechanical alignment strategy. Subsequently, the femoral bone cuts were created corresponding to the internal implant interface using modelling software (SimLab 2019.1, Altair Engineering, Troy, MI, USA). Meshing software was used to create FE models of both the femur and femoral component consisting of linear tetrahedral elements with an edge size of 2.5 mm, based on previous mesh convergence studies (Hypermesh 2017, Altair Engineering, Troy, MI, USA) [10]. As a result, the femur consisted of 67,948 elements and 12,709 nodes and the femoral component of 16,255 elements and 3,883 nodes.

A calibration phantom (0, 50, 100, 200 mg/ml calcium hydroxyapatite, Image Analysis), scanned along the cadaveric femur, was used for assignment of the material properties for each bone element. The material properties were defined based on the conversion of the CT Hounsfield Units to calcium values. In a custom user subroutine, these calcium values were converted to the Young's modulus [11]. The bone was defined as an elastic-plastic material.

The implant was defined as an elastic isotropic material and assigned with a Young's modulus of 3.7 GPa for PEEK-OPTIMA™ given by the manufacturer (Invibio Ltd, Thornton Cleveleys, Lancashire, United Kingdom).

The titanium inlay was modelled using 3D shell elements with a zero thickness, and were fixed to the inner surface of the femoral component. Thickness and stiffness properties for the corresponding titanium inlay variant were subsequently assigned to the shell elements.

The contact between the bone and the implant was modelled using a single-sided touching contact algorithm. The coefficient of friction was set for all variants at 0.5 to evaluate an average value of coefficient of friction [12]. A coulomb bilinear (displacement) friction model was used to define the friction.

The interference fit was numerically specified through the contact algorithm between the bone and the implant at the distal, anterior, posterior and chamfer sides and was only applied in the micromotion simulations and not in the SED simulations.

An interference fit value of 500 μm was chosen based on previous simulations [8]. The FE simulation was divided in an implantation phase and a loading phase. During the implantation phase, the interference fit was linearly increased until the maximum value in 50 increments. The loads were consecutively applied during the loading phase. During the loading phase, the maximum value of the interference fit was kept constant. The variation in inlay thickness did not influence the applied interference fit.

The models were subjected to a jogging loading configuration, which was chosen as a high-load activity for the evaluation of the primary fixation, and was taken from the Orthoload database [13]. The jogging loads were applied as two point loads at the centre of the medial and lateral femoral condyles in the axial direction, defining the tibiofemoral contact forces. Considering the frictionless contact, the anteroposterior and mediolateral components of the forces were assumed negligible. The axial force was separated into a medial and lateral axial force using the medial force ratio from the Orthoload database [14]. A quasi-static simulation was performed in which the loads were incrementally applied in a sequence of 12 increments. Six increments were used to move from the starting situation without loading to the maximum load, and six increments were used to move back to the situation without loads. This represented one loading cycle. Four loading cycles were simulated to allow the implant to settle (numerically). The results were taken from the final loading cycle [10]. As a constraint, a fixed displacement in all directions was applied on the proximal side of the femur.

Five different variations of FE models with a titanium inlay were analysed. The PEEK implant material model was first simulated with a uniform thin, medium, and thick titanium inlay. Additionally, two FE models with titanium inlay variants were created: a thin inlay at the anterior flange and posterior condyles, and a thick inlay distally and at the chamfers, and vice versa (Fig. 3). The proximal and distal region were modelled with a different inlay thickness separately as previous research showed that the anterior flange and posterior condyles are the regions with the largest micromotions [8,10]. The strain values are, however, typically larger in the distal region than the proximal region of the femur [1]. Therefore, a thin inlay at the proximal region and a thick inlay at the distal region of the femoral component and vice versa were analysed.

As outcome measures the micromotions and strain energy for all simulations were calculated.

2.4. Micromotions

For quantification of the primary fixation, the micromotions, defined as the in-plane relative displacements at the contact interface between the implant and the bone in the shearing direction, were defined. Therefore, the nodes on the implant interface were defined as well as the corresponding contact face on the bone interface. The largest distance in the in-plane direction between the contact node on the implant interface and the closest contact face on the bone was calculated for all nodes during the fourth loading cycle in the loading phase, defined as the resulting micromotions. The regions of the pegs and the regions having a large overhang, for example at the posterior condyles and anterior flange, were not included in the results. The 95th percentile of the maximum resulting micromotions was defined for each FE model. This value was defined to remove any possible micromotion outliers in the model.

2.5. Strain energy

For the quantification of stress-shielding, the SED was calculated in each FE model. SED is an accepted stimulus for bone remodelling, with bone resorption being caused by a decrease in SED, relative to the reference case [15,16]. The SED of the reconstruction with an all-PEEK femoral component without an inlay was taken as the reference case, in order to quantify the impact of the titanium inlay. The total strain energy was defined as the SED per element multiplied by the element volume, summed for the whole periprosthetic bone. The strain energy difference was defined as the total strain energy of the femoral reconstruction with the initial all-PEEK femoral component subtracted from the femoral reconstruction with the PEEK component with a titanium inlay. A negative strain energy difference leads to a decrease in strain energy compared to the femoral reconstruction with the all-PEEK femoral component which therefore has a negative impact on the bone remodelling. Regions of interest (ROI) were defined according to similar models from literature to identify the regions with the largest strain energy differences [1].

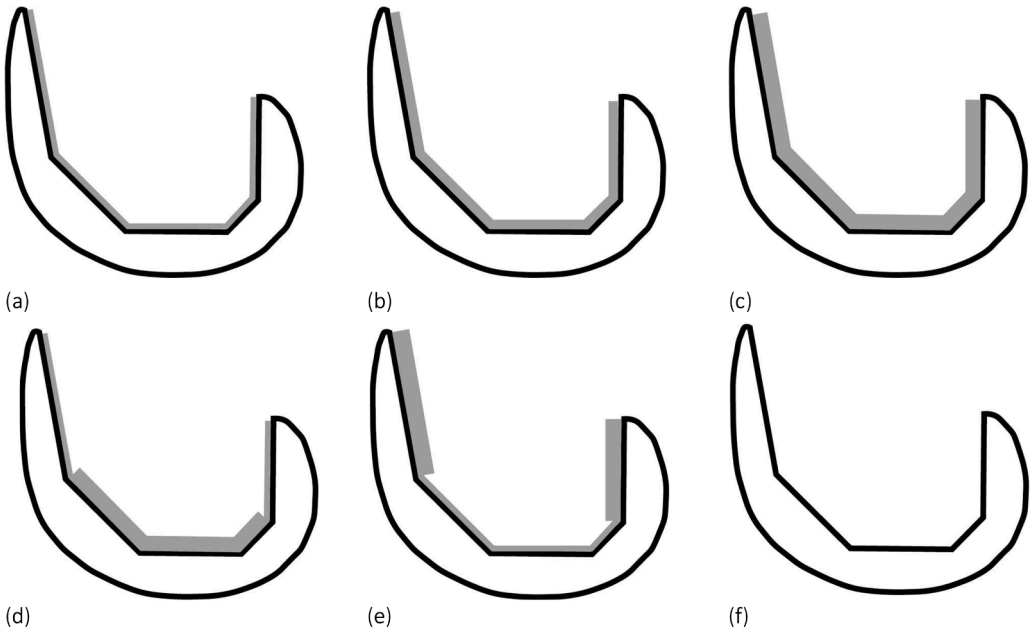

Fig. 3. Titanium inlay variants. (**a**) Uniform thin titanium inlay; (**b**) Uniform medium titanium inlay; (**c**) Uniform thick titanium inlay; (**d**) Distal thick – proximal thin; (**e**) Distal thin – proximal thick; (**f**) All-PEEK femoral component without titanium inlay.

3. Results

3.1. Experimental three-point bending tests

As expected, the largest mean representative Young's modulus value was found for the thick titanium inlay (Table 2).

3.2. Micromotions

The addition of a titanium inlay reduced the micromotions with 30 % to 40 % compared to the all-PEEK femoral component. In all models the largest micromotion values were seen on the medial side of the anterior flange (Fig. 4). After the all-PEEK femoral component, the distal thin – proximal thick variant showed the largest resulting micromotions (Table 3). The micromotion values at the distal and chamfer regions decreased with increasing inlay thickness and stiffness. A thick inlay at the distal and chamfer regions resulted in lower micromotions than a thin inlay at the distal and chamfer regions.

3.3. Strain energy density visualization

The SED decreased mainly in the distal region with the addition of an inlay (Fig. 5). This decrease was more pronounced for the inlays with high stiffness and thickness values.

3.4. Strain energy difference

The addition of a titanium inlay resulted in a decrease in the strain energy. For the total ROI, the difference in strain energy of the PEEK component including titanium inlay compared with the all-PEEK femoral component is 6 % to 10 %. The largest strain energy differences were found in the medial distal region, ROI 2 and ROI 4, for all inlay types. The largest strain energy differences compared to the all-PEEK femoral component were found for the thick inlay with a high stiffness and thickness (Fig. 6).

Table 2
Mean representative Young's modulus per Titanium inlay type.

Titanium inlay type	Mean representative Young's modulus (GPa) (mean ± SD)	Global thickness (mm)
Thin	14.35 ± 0.3775	1.5
Medium	17.34 ± 1.1905	1.7
Thick	24.74 ± 1.7030	2.2

4. Discussion

The objective of the current study was to investigate the effect of the thickness and stiffness of a titanium inlay on the primary fixation, quantified by the micromotions, and on the stress-shielding, quantified by the SED, using FE models. Both outcome measures were sensitive to the presence of a titanium inlay, although the subsequent effects of the different variants investigated were relatively small.

De Ruiter et al. studied the stress-shielding of a cemented PEEK femoral component compared to the stress-shielding of a cemented CoCr femoral component [1]. Their study found that the strain patterns of the femur including a PEEK implant more closely resembles the intact femur than the femur including a CoCr implant. SED differences were more pronounced in the distal and anterior regions at the implant interface and less pronounced in the posterior region. This corresponds with the current results in which the largest strain energy differences were seen in the medial distal region. Similarly, in the current study a PEEK implant with a thick (and hence a stiff) titanium inlay resulted in a larger strain energy difference than a PEEK implant with a thin titanium inlay, although the differences in strain energy difference are small amongst the inlay variants.

The addition of a titanium inlay resulted in a decrease in the micromotions. The micromotion values of the cementless PEEK femoral component including titanium inlay variants that were investigated in the current study were in the same range as the micromotion values of cementless CoCr femoral components investigated previously (20–70 μm) [8]. Although, like the strain energy difference values, the differences in micromotion values amongst the inlay variants are small [10,17]. However, the micromotion values found in the current study were all below the reported micromotion threshold for bone ingrowth (40 - 50 μm) [18,19].

Several studies reported on the use of a surface coating to improve osseointegration of cementless TKA components [9,20]. The study of Aerts et al. investigated the effect of fibre size and porosity on the

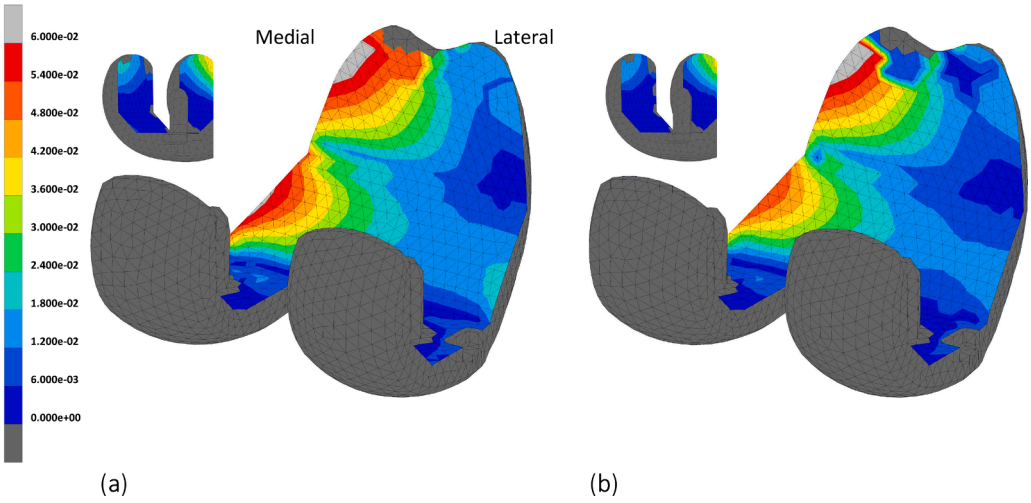

Fig. 4. Resulting micromotion (mm) distribution at the implant interface after the 4th loading cycle. (**a**) PEEK femoral component including uniform thin titanium inlay. (**b**) PEEK femoral component including distal thick – proximal thin titanium inlay.

Table 3
95th percentile of maximum resulting micromotions (μm).

All-PEEK	Thin	Medium	Thick	Distal thick – proximal thin	Distal thin – proximal thick
69.5	51.0	48.9	49.8	43.0	51.2

stiffness of a titanium fibre mesh [9]. As a conclusion, changing the stiffness could effectively be achieved by adapting the fibre size and porosity. The study of Ryu, et al. showed that a titanium porous coating is biocompatible to use as a surface coating of cementless TKA components [20]. Moreover, the contact area between the bone and the implant was larger for the sample including a titanium coating compared with the smooth sample without a coating. These studies suggest that the use of titanium coatings may improve the primary fixation of cementless TKA components. This was confirmed by our study, showing decreased micromotion values in models including a titanium inlay compared with models without an inlay.

Our simulations showed that the addition of a titanium inlay resulted in a decrease in micromotion values, although the effect on the micromotions amongst the inlay variants is relatively small. This therefore allows for further design and development of a titanium inlay on the inner implant interface with an improved primary fixation of the femoral component as result. Especially the use of a thick inlay on the distal side reduces the micromotions and therefore the risk of poor primary fixation of the implant. Nonetheless, we would recommend further research with mechanical experiments to confirm the in this study simulated results. Additionally, the osseointegration of an implant including a titanium inlay may be investigated by assessing the osteoblast viability and the contact between the bone and the implant including a titanium inlay.

There are a few limitations in this study that could be improved in future research. The first limitation is that only one loading condition was investigated in this study, which also only included the tibiofemoral forces. Previous studies have shown that variations in loading conditions may influence the strain in the femur [3,4]. Additionally, patellofemoral forces could also be of interest, particularly for a more flexible implant material such as PEEK. A second limitation is the alignment of the femoral component. Alignment variations influence the load transfer from femur to tibia, and therefore will also affect the strain distribution in the femur. Including loading configurations for more alignment conditions may therefore provide more robust results, although the relative results will not be influenced. Another limitation is that only one bone geometry with corresponding bone density distribution was analysed in this study. A population study including patient variations and surgical variations as cutting errors would result in models with varying bone density distributions and could therefore influence the SED in the bone models. Therefore, this study may be further assessed in a larger

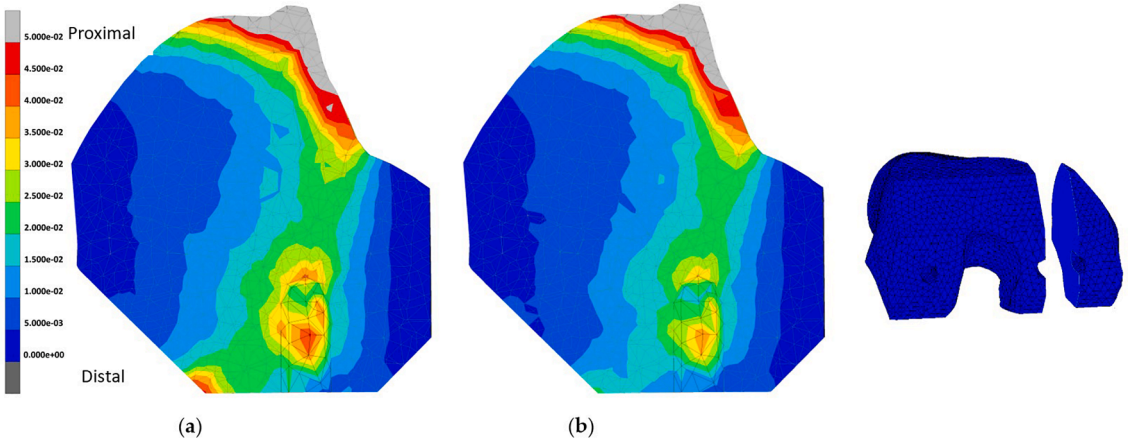

Fig. 5. Total SED (MPa), cutting plane through the medial peg. (**a**) All-PEEK femoral component without titanium inlay; (**b**) PEEK femoral component with uniform thick titanium inlay.

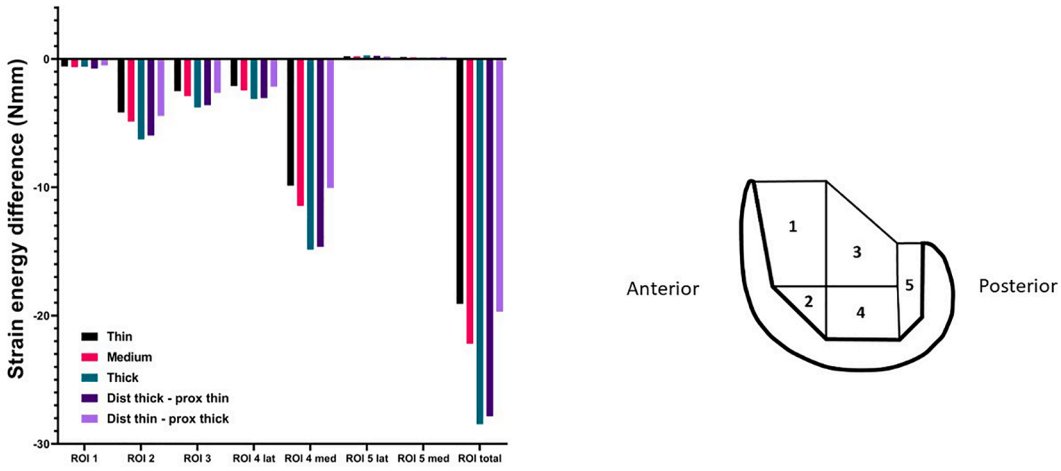

Fig. 6. Strain energy difference (Nmm) per ROI for the three uniform titanium inlay types and two variants with respect to the all-PEEK femoral component without titanium inlay. The ROI total is the sum of the strain energy difference of all ROIs.

population of models. Another limitation is that the titanium inlay has been modelled as a solid layer in the FE models, while the inlay consists of a solid core layer and two porous outer layers sintered together. However, this was accounted for by modelling the average representative Young's modulus. Finally, the inlays were simulated with zero thickness elements, which would be different from the actual physical specimens. Although the structural stiffness (e.g. shell thickness) was incorporated in the FEA models, in the clinical or experimental situation the titanium inlay would have a physical thickness, which was not included. For implants with an inlay, it is the intention to maintain the same internal dimensions for the femoral component, which means the inlay would take up space of the PEEK material. However, due to the porous structure the inlay would also partially be infused with PEEK during the manufacturing. The effects of an infused titanium inlay on the structural stiffness should be further investigated to evaluate the primary stability of actual end products. In addition, since the porosity was not physically modelled in the models, any change in porosity or composition of the inlay would require additional experimental testing to ensure that the structural stiffness (i.e. second moment of inertia) is correctly reflected by the shell elements.

In conclusion, adding an inlay to the PEEK femoral component led to a decrease in micromotions when compared to the all-PEEK component. Only small differences were seen between the different inlay variations. Adding an inlay only had a minor effect on the SED distribution as compared to the all-PEEK implant, with the largest decrease seen in the most distal region.

Funding

This study was funded by Invibio Ltd., Lancashire, United Kingdom. Invibio Ltd. was not involved in the collection, analysis and interpretation of the data.

Ethical approval

Not required.

Declaration of Competing Interest

The authors declare the following financial interests/ personal relationships which may be considered as potential competing interests: A. B. is a paid employee of Invibio Ltd. and had a role in the study design and review of the manuscript. N.V. is a paid consultant for Invibio Ltd. D.J. is a paid consultant for Invibio Ltd. and receives research support as a principal investigator from Invibio Ltd. The other authors declare no conflict of interest.

Acknowledgments

INVIBIO^{TM}, PEEK-OPTIMA^{TM}, INVIBIO BIOMATERIAL SOLUTIONS^{TM} are trademarks of Victrex plc. Implant geometry was supplied by Maxx Orthopedics Inc. No writing assistance was provided for writing this manuscript.

References

[1] de Ruiter L, et al. Decreased stress shielding with a PEEK femoral total knee prosthesis measured in validated computational models. J Biomech 2021;118:110270.
[2] Petersen MM, et al. Decreased bone density of the distal femur after uncemented knee arthroplasty. A 1-year follow-up of 29 knees. Acta Orthop Scand 1996;67(4):339–44.
[3] de Ruiter L, et al. The mechanical response of a polyetheretherketone femoral knee implant under a deep squatting loading condition. Proc Inst Mech Eng H 2017;231(12):1204–12.
[4] de Ruiter L, et al. A preclinical numerical assessment of a polyetheretherketone femoral component in total knee arthroplasty during gait. J Exp Orthop 2017;4(1):3.
[5] Dalury DF. Cementless total knee arthroplasty. Bone Joint J 2016;98-B(7):867–73.
[6] Meneghini RM, Hanssen AD. Cementless fixation in total knee arthroplasty: past, present, and future. J Knee Surg 2008;21(4):307–14.
[7] Prudhon JL, Verdier R. Cemented or cementless total knee arthroplasty? - Comparative results of 200 cases at a minimum follow-up of 11 years. SICOT J, 2017;3:70.
[8] Post CE, et al. A FE study on the effect of interference fit and coefficient of friction on the micromotions and interface gaps of a cementless PEEK femoral component. J Biomech 2022;137:111057.
[9] Aerts E, et al. Porous titanium fiber mesh with tailored elasticity and its effect on stromal cells. J Biomed Mater Res B Appl Biomater 2020;108(5):2180–91.
[10] Berahmani S, et al. FE analysis of the effects of simplifications in experimental testing on micromotions of uncemented femoral knee implants. J Orthop Res 2016;34(5):812–9.
[11] Keyak JH, et al. Predicting proximal femoral strength using structural engineering models. Clin Orthop Relat Res 2005;(437):219–28.
[12] Shirazi-Adl A, Dammak M, Paiement G. Experimental determination of friction characteristics at the trabecular bone/porous-coated metal interface in cementless implants. J Biomed Mater Res 1993;27(2):167–75.
[13] Bergmann G, et al. Standardized loads acting in knee implants. PLoS ONE 2014;9(1):e86035.
[14] Kutzner I, et al. Mediolateral force distribution at the knee joint shifts across activities and is driven by tibiofemoral alignment. Bone Joint J 2017;99-B(6):779–87.
[15] Carter DR, Fyhrie DP, Whalen RT. Trabecular bone density and loading history: regulation of connective tissue biology by mechanical energy. J Biomech 1987;20(8):785–94.
[16] Huiskes R, et al. Adaptive bone-remodeling theory applied to prosthetic-design analysis. J Biomech 1987;20(11–12):1135–50.
[17] Berahmani S, Janssen D, Verdonschot N. Experimental and computational analysis of micromotions of an uncemented femoral knee implant using elastic and plastic bone material models. J Biomech 2017;61:137–43.

[18] Engh CA, et al. Quantification of Implant Micromotion, Strain Shielding, and Bone Resorption With Porous-Coated Anatomic Medullary Locking Femoral Prostheses. Clin Orthop Relat Res 1992;285:13–29.
[19] Jasty M, et al. In vivo skeletal responses to porous-surfaced implants subjected to small induced motions. J Bone Joint Surg 1997;79(5):707–14.
[20] Ryu DJ, et al. Osteo-compatibility of 3D titanium porous coating applied by direct energy deposition (DED) for a cementless total knee arthroplasty implant: in vitro and in vivo study. J Clin Med 2020;9(2).